DEVELOPMENT OF A NEUTRON NOISE SIMULATOR FOR HEXAGONAL GEOMETRIES

A. Vidal-Ferràndiz[1], **A. Carreño**[1], **D. Ginestar** [1], **G. Verdú**[1]
[1] Universitat Politècnica de València,
Camí de Vera s/n, 46022, València, Spain

anvifer2@upv.es, amcarsan@iqn.upv.es, dginesta@mat.upv.es, gverdu@iqn.upv.es

dx.doi.org/10.13182/M&C21-33654

ABSTRACT

The study of neutron flux fluctuations permits to detect anomalies during the operation of nuclear reactors. To effectively use this technique for nuclear reactor diagnostics, it is essential to accurately model the effects of the different types of anomalies on the neutron flux field. This paper deals with the development and validation of a neutron noise simulator for reactors with any kind of geometry, that is, rectangular and hexagonal geometries. The neutron noise can be obtained by a frequency-domain or a time-domain methodology. In this work we compare both methodologies in hexagonal reactors. The time-domain analysis solves the time-dependent neutron diffusion equation and then performs a Fourier analysis of the obtained time-dependent neutron fluxes and it is usually used as reference. On the other hand, the frequency-domain methodology solves the frequency-domain first-order neutron noise equation with complex values. To show the possibilities of the neutron noise simulator developed a generic absorbers of variable strength perturbation inside a three-dimensional hexagonal reactor is investigated. Both methodologies show similar numerical results.

KEYWORDS: Neutron noise; Finite element method; Frequency-domain analysis, Hexagonal geometry

1. INTRODUCTION

Being able to monitor the state of nuclear reactors while they are running at nominal conditions is a safety requirement. The early detection of anomalies gives the possibility to take proper actions before such problems lead to safety concerns or impact in the plant availability. [1]. To be able to detect, localize and quantify a perturbation in real-time, an automatic algorithm based on machine learning has to be provided with a large set of simulation data [2].

One useful technique to solve the effect of a perturbation in the neutron noise is to resolve the frequency-domain first-order neutron noise equation in the diffusion approximation [3]. This equation must be solved after finding the steady state of the reactor because the static neutron flux for the different energy groups are variables of this equation. The first order noise equation is derived by subtracting the static equations the time-dependent ones and considering small fluctuations compared to the mean values. Finally, a Fourier transform is performed. The frequency-domain methodology requires to solve a large linear system with complex values. This methodology has been applied to rectangular [4] [5] and hexagonal reactors [6].

On the other hand, the time-domain methodology is based in solving the time-dependent neutron diffusion equation over a perturbed transitory and perform a numerical discrete Fourier transform to compare the obtained results with the frequency-domain analysis. The main advantage of this methodology is that it does not imply any approximation. However, this methodology needs to solve accurately a linear system each time step where the change in the neutron flux is quite small.

Other approximations to the neutron transport equation have been also applied to neutron noise simulations as Montecarlo calculation [7]. Other works have used deterministic strategies as the method of characteristic [8] and the SP_3 approximation.

This work presents a neutron noise simulator in the frequency domain developed with the finite element method (FEM), called `FEMFFUSION-FD` and compares its results with the time-domain methodology presented in [9] and in [10]. These codes are an extension of the open source neutron diffusion solver `FEMFFUSION` [11].

The reset of the manuscript is organizes as follows. Section 2 describes the finite element discretization of the neutron diffusion equation in its steady state version. Section 3 describes the first order neutron noise equation in the frequency domain. Then, Section 4 compares numerically the time-domain an frequency-domain methodologies in a hexagonal reactor. The conclusions of the work are described in Section 5.

2. FEM DISCRETIZATION OF THE NEUTRON DIFFUSION EQUATION

In the 2-group theory, the time-dependent neutron diffusion equation with one group of delayed neutrons, where the matrices are denoted by $[\,]$, is defined as [12]

$$[\mathrm{v}^{-1}]\frac{\partial \phi}{\partial t} - \vec{\nabla}\cdot\left([D]\vec{\nabla}\phi\right) + [\Sigma_T]\phi = (1-\beta_{\text{eff}})\chi[\nu\Sigma_f]^T\phi + \lambda_{\text{eff}}\chi\mathcal{C}, \tag{1}$$

$$\frac{\partial \mathcal{C}}{\partial t} = \beta_{\text{eff}}[\nu\Sigma_f]^T\Phi - \lambda_{\text{eff}}\mathcal{C}, \tag{2}$$

where the material dependent matrices are defined as

$$[\mathrm{v}^{-1}] = \begin{bmatrix} \frac{1}{\mathrm{v}_1} & 0 \\ 0 & \frac{1}{\mathrm{v}_2} \end{bmatrix}, \qquad [\Sigma_T] = \begin{bmatrix} \Sigma_{a1}+\Sigma_{12} & 0 \\ -\Sigma_{12} & \Sigma_{a2} \end{bmatrix},$$

$$[D] = \begin{bmatrix} D_1 & 0 \\ 0 & D_2 \end{bmatrix}, \qquad [\nu\Sigma_f] = \begin{bmatrix} \nu\Sigma_{f1} \\ \nu\Sigma_{f2} \end{bmatrix}, \quad \chi = \begin{bmatrix} 1 \\ 0 \end{bmatrix}.$$

The main unknown of the neutron transport equation is the space- and time dependent neutron flux, in its usual separation in the fast and thermal energy groups $\phi = \begin{bmatrix}\phi_1, & \phi_2\end{bmatrix}^T$. All other quantities have their usual meaning in the nuclear engineering field [12].

2.1. STATIC PROBLEM

For a given transient analysis in a core reactor, as a neutron noise simulation, a static configuration of the reactor is considered as initial condition. Associated with the time dependent neutron

diffusion equation, (1) and (2), there is the static diffusion equation given by

$$-\vec{\nabla}\cdot([D]\vec{\nabla}\phi+[\Sigma_T]\phi=\frac{1}{k_{\text{eff}}}\chi(\nu\Sigma_f)^T\phi. \tag{3}$$

This is a eigenvalue problem where the fundamental eigenvalue (the largest one) is called the k-effective of the reactor core, and this eigenvalue and its corresponding eigenfunction describe the steady state neutron distribution in the core. In this way, the calculation of the stationary neutron flux distribution is the first step for any neutron noise analysis and other transient analysis.

To solve problem (3), a spatial discretization of the equations has to be selected. In this work, a high order continuous Galerkin finite element method is used [13]. This discretization leads to an algebraic eigenvalue problem associated with the discretization of equation (3) with the following block structure,

$$\begin{bmatrix} L_{11} & 0 \\ -L_{21} & L_{22} \end{bmatrix}\begin{bmatrix} \tilde{\phi}_1 \\ \tilde{\phi}_2 \end{bmatrix}=\frac{1}{\lambda}\begin{bmatrix} M_{11} & M_{12} \\ 0 & 0 \end{bmatrix}\begin{bmatrix} \tilde{\phi}_1 \\ \tilde{\phi}_2 \end{bmatrix}\ , \tag{4}$$

where $\tilde{\phi}_1$ and $\tilde{\phi}_2$ are the algebraic vectors of weights associated with the fast and thermal neutron fluxes. The matrices elements of the different blocks are given by

$$[L_{11}]_{ij}=\sum_{e=1}^{N_e}\left(D_1\int_{\Omega_e}\vec{\nabla}N_i\vec{\nabla}N_j\,\mathrm{d}V-D_1\int_{\Gamma_e}N_i\vec{\nabla}N_j\,\mathrm{d}\vec{S}+(\Sigma_{a1}+\Sigma_{12})\int_{\Omega_e}N_iN_j\,\mathrm{d}V\right), \tag{5a}$$

$$[L_{21}]_{ij}=\sum_{e=1}^{N_e}\Sigma_{12}\int_{\Omega_e}N_iN_j\,\mathrm{d}V, \tag{5b}$$

$$[L_{22}]_{ij}=\sum_{e=1}^{N_e}\left(D_2\int_{\Omega_e}\vec{\nabla}N_i\vec{\nabla}N_j\,\mathrm{d}V-D_2\int_{\Gamma_e}N_i\vec{\nabla}N_j\,\mathrm{d}\vec{S}+\Sigma_{a2}\int_{\Omega_e}N_iN_j\,\mathrm{d}V\right), \tag{5c}$$

$$[M_{11}]_{ij}=\sum_{e=1}^{N_e}\nu\Sigma_{f1}\int_{\Omega_e}N_iN_j\,\mathrm{d}V, \tag{5d}$$

$$[M_{12}]_{ij}=\sum_{e=1}^{N_e}\nu\Sigma_{f2}\int_{\Omega_e}N_iN_j\,\mathrm{d}V, \tag{5e}$$

where N_i is the prescribed shape function for the i-th node. For simplicity, the shape functions used are Lagrange polynomials that constitute the Lagrange finite elements [13]. Ω_e ($e=1,\ \ldots,\ N_e$) are the reactor subdomains (cells) in which the reactor domain is divided. In the same way, Γ_e are the corresponding subdomain surfaces which are part of the reactor frontier. More details on the spatial discretization used can be found in [14].

To solve the algebraic eigenvalue problem (4) a Krylov-Schur method is used. To accelerate the computation, the generalized eigenvalue problem is reduced to an ordinary eigenvalue problem of the form,

$$L_{11}^{-1}\left(M_{11}+M_{12}L_{22}^{-1}L_{21}\right)\tilde{\phi}_1=\lambda\tilde{\phi}_1\ , \tag{6}$$

which is solved for the dominant eigenvalue (k_{eff}) and its corresponding eigenvector. In this way, for each matrix-vector product it is necessary to solve two linear systems associated with L_{11} and L_{22}, to avoid the calculation of their inverse matrices. These linear systems are solved by

means of an iterative scheme as the preconditioned Conjugate Gradient method. Particularly, a Cuthill-McKee reordering is performed to reduce the bandwidth of the matrices, together with an incomplete LU factorization is used for the preconditioning. Also, other efficient solvers has been elaborated as the BIFPAM [9] and Newton iteration solver [15] for the neutron diffusion equation in its steady state form.

3. FIRST-ORDER NEUTRON NOISE THEORY

The first-order neutron noise theory is based on splitting every time dependent term, expressed as $X(\vec{r}, t)$, into their mean value, X_0, which is considered as the steady-state solution, and their fluctuation around the mean value, δX as

$$X(\vec{r},\, t) = X_0(\vec{r}) + \delta X(\vec{r},\, t). \tag{7}$$

The fluctuations are assumed to be small compared to the mean values. This allows to neglect second-order terms $(\delta X(\vec{r},\, t) \times \delta X(\vec{r},\, t)) = 0$. Also, the fluctuations of the diffusion coefficients are neglected and $\delta D_g = 0$ is assumed. Thus, the first-order neutron noise equation in the frequency-domain can be written as [3] [5].

$$-\vec{\nabla} \cdot \left(D\vec{\nabla}\delta\phi(\vec{r},\, \omega) \right) + [\Sigma_{\text{dyn}}]\, \delta\phi(\vec{r},\, \omega) = \delta S(\vec{r},\, \omega), \tag{8}$$

where ω is the frequency variable and $\vec{r}$ de position variable. The perturbation source term $\delta S(\vec{r},\, \omega)$ is given by the frequency-domain changes in the materials cross sections:

$$\delta S(\vec{r},\, \omega) = \begin{bmatrix} \delta S_1(\vec{r},\, \omega) \\ \delta S_2(\vec{r},\, \omega) \end{bmatrix} = [\phi_s]\, \delta\Sigma_{12} + [\phi_a] \begin{bmatrix} \delta\Sigma_{a1} \\ \delta\Sigma_{a2} \end{bmatrix} + \frac{1}{k_{\text{eff}}} [\phi_f] \begin{bmatrix} \delta\nu\Sigma_{f1} \\ \delta\nu\Sigma_{f2} \end{bmatrix}, \tag{9}$$

where

$$[\Sigma_{\text{dyn}}] = \begin{bmatrix} \Sigma_1 & -\nu\Sigma_{f2} \left(1 - \frac{j\omega\beta_{\text{eff}}}{j\omega + \lambda_{\text{eff}}} \right) \\ -\Sigma_{12} & -\Sigma_{a2} + \frac{j\omega}{\text{v}_2} \end{bmatrix}, \qquad [\phi_s] = \begin{bmatrix} -\phi_1 \\ \phi_1 \end{bmatrix},$$

$$[\phi_a] = \begin{bmatrix} \phi_1 & 0 \\ 0 & \phi_2 \end{bmatrix}, \qquad [\phi_f] = \left(1 - \frac{j\omega\beta_{\text{eff}}}{j\omega + \lambda_{\text{eff}}} \right) \begin{bmatrix} \phi_1 & \phi_2 \\ 0 & 0 \end{bmatrix},$$

$$\Sigma_1 = \Sigma_a + \frac{j\omega}{\text{v}_1} + \Sigma_{12} - \nu\Sigma_{f1} \left(1 - \frac{j\omega\beta_{\text{eff}}}{j\omega + \lambda_{\text{eff}}} \right).$$

By comparing equation (3), it can be seen that the neutron noise equation is an in-homogeneous equation with complex quantities that has to be solved after the steady-state solution is obtained because ϕ_1 and ϕ_2 represent the steady state fast and thermal neutron fluxes, respectively. The related static eigenvalue problem must be solved with the same spatial discretization as the frequency domain neutron noise equation to get coherent results.

Applying the continuous Galerkin finite element discretization to Eq. (8) leads to an algebraic linear system of equation with the following block structure

$$\begin{bmatrix} A_{11} & A_{12} \\ A_{21} & A_{22} \end{bmatrix} \delta\tilde{\Phi} = \begin{bmatrix} S_1 \\ S_2 \end{bmatrix}, \tag{10}$$

where $\delta\tilde{\Phi} = \left[\delta\tilde{\phi}_1,\ \delta\tilde{\phi}_2\right]^T$ are the algebraic vectors of weights associated with the fast and thermal neutron noise fluxes. The matrices elements of the different blocks are given by

$$[A_{11}]_{ij} = \sum_{e=1}^{N_e}\left(D_1\int_{\Omega_e}\vec{\nabla}N_i\vec{\nabla}N_j\,\mathrm{d}V - D_1\int_{\Gamma_e}N_i\vec{\nabla}N_j\,\mathrm{d}\vec{S} + [\Sigma_{\text{dyn}}]_{11}\int_{\Omega_e}N_iN_j\,\mathrm{d}V\right)\ , \tag{11a}$$

$$[A_{12}]_{ij} = \sum_{e=1}^{N_e}[\Sigma_{\text{dyn}}]_{12}\int_{\Omega_e}N_iN_j\,\mathrm{d}V\ , \tag{11b}$$

$$[A_{21}]_{ij} = \sum_{e=1}^{N_e}[\Sigma_{\text{dyn}}]_{21}\int_{\Omega_e}N_iN_j\,\mathrm{d}V\ , \tag{11c}$$

$$[A_{22}]_{ij} = \sum_{e=1}^{N_e}\left(D_2\int_{\Omega_e}\vec{\nabla}N_i\vec{\nabla}N_j\,\mathrm{d}V - D_2\int_{\Gamma_e}N_i\vec{\nabla}N_j\,\mathrm{d}\vec{S} + [\Sigma_{\text{dyn}}]_{22}\int_{\Omega_e}N_iN_j\,\mathrm{d}V\right)\ , \tag{11d}$$

$$[S_1]_{ij} = \sum_{e=1}^{N_e}\int_{\Omega_e}\delta S_1(\vec{r},\omega)\,N_iN_j\,\mathrm{d}V\ , \tag{11e}$$

$$[S_2]_{ij} = \sum_{e=1}^{N_e}\int_{\Omega_e}\delta S_2(\vec{r},\omega)\,N_iN_j\,\mathrm{d}V\ . \tag{11f}$$

4. NUMERICAL RESULTS

As a case of study, a usual three-dimensional hexagonal VVER-1000 reactor core is considered [6]. This benchmark has a 1/12 reflective symmetry but as the inserted perturbation is not symmetrical, the whole reactor must be solved. The core is composed of 163 fuel assemblies surrounded by 54 reflector cells. Figure 1 shows the materials layout of the core. The fuel assembly pitch is 23.6 cm and the active height is 355 cm. Therefore, the total height is 426 cm including 35.5 cm thick reflectors in the upper and the lower part of the core. The reactor is discretized into 24 planes, each one of 17.75 cm thick.

A generic absorber of variable strength perturbation is inserted in the fuel assembly marked with a cross ($\times$) in Figure 1 on the plane 12 of 10% of the value of Σ_{a1} and Σ_{a2} cross sections, $\delta\Sigma_{a1} = 1.06731\times10^{-3}$ cm^{-1} and $\delta\Sigma_{a2} = 8.85869\times10^{-3}$ cm^{-1}. The cross section data of this benchmark is shown in Table 1. Kinetic data of this benchmark problem is shown in Table 2. Vacuum boundary conditions have been considered for this benchmark.

To compare the different solutions computed, we have defined the following error indicators:

$$\Delta k_{\text{eff}} = k_{\text{eff}} - k_{\text{eff}}^{\text{ref}},$$

$$\varepsilon_g = 100\times\frac{1}{N_c}\sum_{c=1}^{N_c}\frac{\phi_{c,g}-\phi_{c,g}^{\text{ref}}}{\phi_{c,g}^{\text{ref}}}\ \%, \qquad g = 1,\ 2,$$

$$\zeta_g = 100\times\frac{1}{N_c}\sum_{c=1}^{N_c}\frac{|\delta\phi_{c,g}| - \left|\delta\phi_{c,g}^{\text{ref}}\right|}{\left|\delta\phi_{c,g}^{\text{ref}}\right|}\ \%, \qquad g = 1,\ 2,$$

$$\eta_g = 100 \times \frac{1}{N_c} \sum_{c=1}^{N_c} \frac{\arg(\delta\phi_{c,g}) - \arg(\delta\phi_{c,g}^{\text{ref}})}{\arg(\delta\phi_{c,g}^{\text{ref}})} \ \%, \qquad g = 1,\ 2,$$

where values with the superscript $^{\text{ref}}$ represent reference results extracted with an accurate time-domain calculation obtained with a refined mesh and a fifth polinomial degree in the finite element method FED $= 5$ and $\Delta t = 10^{-3}$ s. $\phi_{c,g}^{\text{ref}}$ and $\delta\phi_{c,g}^{\text{ref}}$ are the steady-state mean flux and the average noise flux, respectively, at the hexagonal cell c. N_c is the number of hexagonal cells in the reactor.

Table 3 shows the static results for the VVER-1000 benchmark for different depending on the polynomial degree used in the FEM shape functions (FED). As we use the same code to calculate the steady-state of the reactor, the steady-state results for the frequency-domain and timer-domain methodologies are the same. Table 4 compares the time-domain and the frequency-domain methodologies employed and the FED ranging from 1 to 3. This Table shows that the differences between the frequency-domain and time-domain methodology using the same FED are small, validating both methodologies. Also, it can be seen that calculations with linear shape functions do not provide accurate enough results. The FED $= 2$ and FED $= 3$ provide accurate results for this benchmark. Also, it can be observed that the static results show smaller errors that the neutron noise results with the same discretization. This indicates that finer meshes must be used in noise simulations to ensure accurate results.

Figure 2 represents the middle plane ($z = 177.5$ cm) of the static assembly flux values for the steady state solution using FED $= 3$. Figure 3 presents the neutron noise magnitude obtained with FED $= 3$ and the frequency-domain approach. The results show that the thermal neutron noise is mostly localized while the fast neutron noise has influence over a wider region. Figure 4 shows the neutron noise phase results. The phase of the neutron noise is similar throughout the entire reactor.

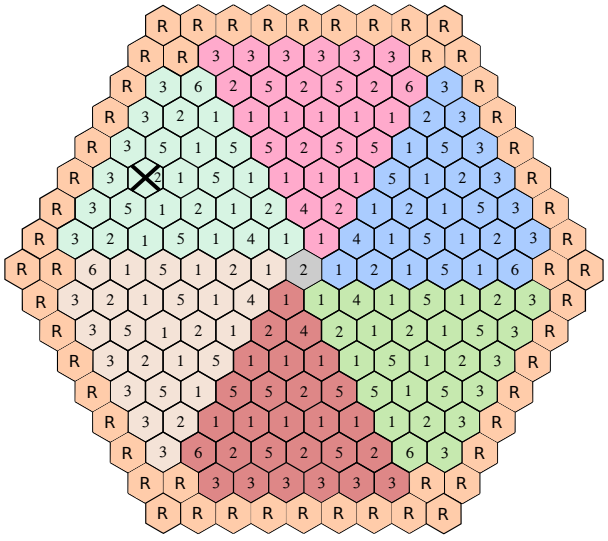

Figure 1: Material layout of the VVER-1000 reactor.

Table 1: Cross section data for VVER-1000 reactor.

Material	Group	$\Sigma_{tr,g}$ (1/cm)	Σ_{ag} (1/cm)	$\nu\Sigma_{fg}$ (1/cm)	Σ_{12} (1/cm)
1	1	2.48450e–1	1.00950e–2	5.39871e–3	1.11009e–2
	2	7.18780e–1	7.04091e–2	9.52272e–2	
2	1	2.47824e–1	1.06731e–2	6.66620e–3	1.07324e–2
	2	7.30392e–1	8.85869e–2	1.34809e–1	
3	1	2.43091e–1	1.11765e–2	8.13314e–3	1.14067e–2
	2	7.70401e–1	1.09003e–1	1.78327e–1	
4	1	2.32926e–1	9.63601e–3	5.86762e–3	1.42223e–2
	2	8.17510e–1	8.41074e–2	1.10340e–1	
5	1	2.32849e–1	9.75808e–3	5.86196e–3	1.41352e–2
	2	8.21538e–1	8.77763e–2	1.10451e–1	
6	1	2.32238e–1	1.04844e–2	7.40621e–3	1.39202e–2
	2	8.33502e–1	1.04848e–1	1.52190e–1	
R	1	2.07775e–1	4.71403e–4	0.00000e–0	4.19586e–2
	2	1.33650e–1	1.20450e–2	0.00000e–0	

β_{eff}	λ_{eff} (s^{-1})	v_1 (cm s^{-1})	v_2 (cm s^{-1})
0.0065	0.0767	1.8230e+7	4.1306e+5

Table 2: Kinetic data for the 3D VVER-1000 benchmark problem.

5. CONCLUSIONS

This work presents a neutron noise simulator developed using the finite element method. It can deal with different kinds of geometry allowing complex domains as hexagonal reactors and any location and shape of the perturbation. Numerical results compare this frequency-domain simulation with a time-domain methodology. The small differences shown in the results validate both the frequency-domain methodology and the time-domain methodology against a generic absorber of variable strength in a selected location. These codes could permit to train machine learning algorithms to detect and quantify perturbations in real-time in operating nuclear reactors of any type of geometry.

ACKNOWLEDGEMENTS

The research leading to these results has received funding from the Euratom research and training programme 2014-2018 under grant agreement No 754316.

Methodology	FED	DoFs	k_{eff}	Δk_{eff} (pcm)	ε_1 (%)	ε_2 (%)
Time- and Frequency-domain	1	35 150	1.026 03	2036	4.60	6.06
Time- and Frequency-domain	2	265 286	1.008 30	263	0.29	0.45
Time- and Frequency-domain	3	877 898	1.005 95	28	0.11	0.15

Table 3: Comparison table for the steady-state problem of 3D VVER-1000 reactor.

Methodology	FED	ζ_1 (%)	ζ_2 (%)	η_1 (%)	η_2 (%)
Frequency-domain	1	10.51	10.58	0.03	0.03
Frequency-domain	2	1.58	1.58	0.04	0.04
Frequency-domain	3	0.42	0.42	0.04	0.04
Time-domain	1	11.63	11.70	0.02	0.02
Time-domain	2	1.23	1.25	0.00	0.00
Time-domain	3	0.19	0.20	0.00	0.00

Table 4: Comparison table for the neutron noise problem of 3D VVER-1000 reactor.

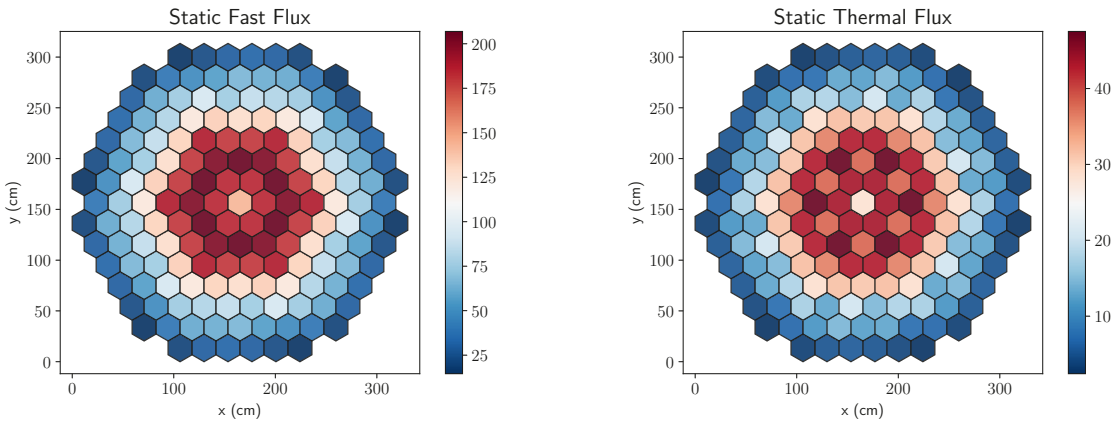

(a) Fast Flux **(b) Thermal Flux**

Figure 2: Static neutron fluxes in the VVER-1000 reactor.

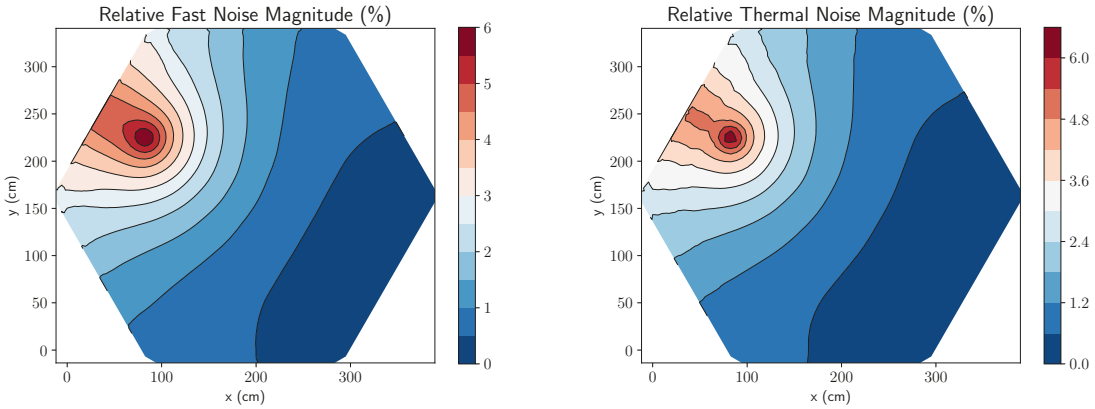

(a) Fast Flux Noise **(b) Thermal Flux Noise**

Figure 3: Magnitude of the noise in the VVER-1000 reactor.

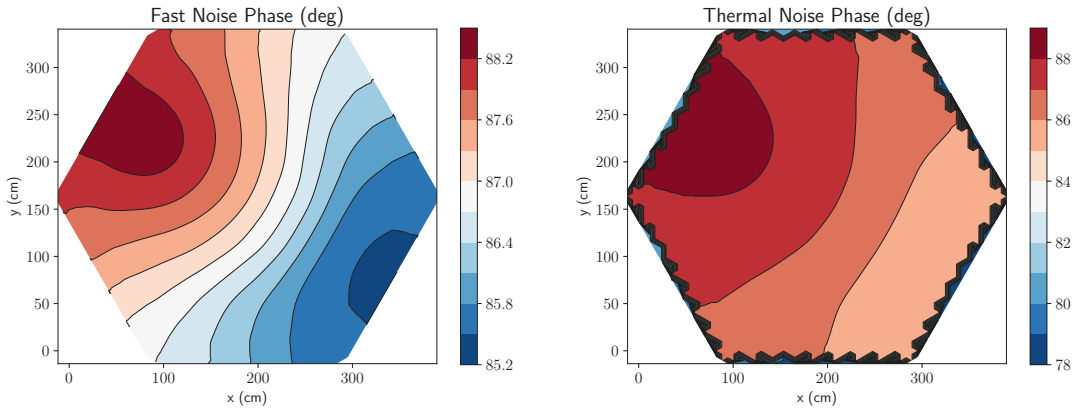

(a) Fast Flux Noise **(b) Thermal Flux Noise**

Figure 4: Phase of the noise in the VVER-1000 reactor.

REFERENCES

[1] C. Demazière, P. Vinai, M. Hursin, S. Kollias, and J. Herb. "Noise-Based Core Monitoring and Diagnostics - Overview of the project." In *Advances in Reactor Physics (ARP-2017)*, pp. 1–4. Mumbai, India (2017).

[2] F. D. S. Ribeiro, F. Caliva, D. Chionis, A. Dokhane, A. Mylonakis, C. Demazière, G. Leontidis, and S. Kollias. "Towards a Deep Unified Framework for Nuclear Reactor Perturbation Analysis." In *2018 IEEE Symposium Series on Computational Intelligence (SSCI)* (2018).

[3] C. Demazière. "CORE SIM: A multi-purpose neutronic tool for research and education." *Ann Nucl Energy*, **volume 38**(12), pp. 2698–2718 (2011).

[4] A. G. Mylonakis, P. Vinai, and C. Demazière. "Numerical solution of two-energy-group neutron noise diffusion problems with fine spatial meshes." *Annals of Nuclear Energy*, **volume 140**, p. 107093 (2020).

[5] A. Mylonakis, P. Vinai, and C. Demazière. "CORE SIM: A flexible diffusion-based solver for neutron noise simulations." *Annals of Nuclear Energy*, **volume 155**, p. 108149 (2021).

[6] H. Malmir and N. Vosoughi. "Propagation noise calculations in VVER-type reactor core." *Progress in Nuclear Energy*, **volume 78**, pp. 10–18 (2015).

[7] T. Yamamoto. "Implementation of a frequency-domain neutron noise analysis method in a production-level continuous energy Monte Carlo code: Verification and application in a BWR." *Ann Nucl Energy*, **volume 115**, pp. 494–501 (2018).

[8] A. Gammicchia, S. Santandrea, I. Zmijarevic, R. Sanchez, Z. Stankovski, S. Dulla, and P. Mosca. "A MOC-based neutron kinetics model for noise analysis." *Annals of Nuclear Energy*, **volume 137**, p. 107070 (2020).

[9] A. Vidal-Ferràndiz, A. Carreño, D. Ginestar, and G. Verdú. "A Block Arnoldi Method for the SP_N Equations." *International Journal of Computer Mathematics*, pp. 1–22 (2019).

[10] A. Vidal-Ferràndiz, A. Carreño, D. Ginestar, C. Demazière, and G. Verdú. "Neutronic Simulation of Fuel Assembly Vibrations in a Nuclear Reactor." *Nuclear Science and Engineering*, **volume 194**(11), pp. 1067–1078 (2020).

[11] "FEMFFUSION a finite element method code for nuclear reactor modelling." https://www.femffusion.imm.upv.es. Accessed: 2022-02-28.

[12] W. M. Stacey. *Nuclear Reactor Physics*. Wiley, Weinheim, Germany (2007).

[13] O. C. Zienkiewicz, R. L. Taylor, and J. Z. Zhu. *The Finite Element Method: Its Basis and Fundamentals*. Butterworth-Heinemann, Oxford, 7th edition (2013).

[14] A. Vidal-Ferràndiz, R. Fayez, D. Ginestar, and G. Verdú. "Solution of the Lambda modes problem of a nuclear power reactor using an h–p finite element method." *Annals of Nuclear Energy*, **volume 72**, pp. 338–349 (2014).

[15] A. Carreño, L. Bergamaschi, A. Martinez, A. Vidal-Ferràndiz, D. Ginestar, and G. Verdú. "Block Preconditioning Matrices for the Newton Method to Compute the Dominant λ-Modes Associated with the Neutron Diffusion Equation." *Mathematical and Computational Applications*, **volume 24**(1), p. 9 (2019).